High-Speed LED Driver for ns-Pulse Switching of High-Current LEDs

Hubert Halbritter, Claus Jäger, Rolf Weber, Michael Schwind, and Frank Möllmer

***Abstract*— This letter analyzes the intrinsic optical switching response of state-of-the-art high power, multiquantum wells, thin-film, and surface-textured infrared light emitting diodes (LEDs). For the switching time response of such devices, the theoretical basics are presented and their predictions are experimentally verified. In the second part of this letter, a novel, fast switching LED driving circuit is presented which enables nanosecond-pulse operation. The circuit reduces significantly the optical rise and fall time of LEDs from 10/15 ns, respectively, down to 2.6 ns at 2-A pulse current without compromising the peak output power.**

***Index Terms*— Light-emitting diode, drive circuit, carrier sweep-out, peaking, time-of-flight, modulation, rise time, fall time, spontaneous emission, multi-quantum-well, large signal modulation, time response.**

I. Introduction

THE advent of high-power infrared light-emitting diodes (IR-LEDs) opens up new application areas. One of them are time-of-flight (TOF) systems for gesture recognition. Key parameters are high optical output power and fast optical rise and fall times to achieve the required performance [1]. Typical pulse widths for these systems are in the range between 5 ns to 50 ns (with 10 MHz to 100 MHz repetition rate) [1], depending on the kind of application. Many systems operating beyond 50 MHz switch to LASER diode based light sources as high-power LEDs are often perceived to have optical rise and fall times too slow for this kind of operation. In the past high-speed LED operation was mainly of interest for plastic optical fiber or - more recently - visible light communication [2]–[4]. This led to the development of special LEDs, either resonant-cavity LEDs or LEDs with doped active layers. Both usually feature a low wall-plug efficiency and also low output power [5]–[7], rendering them unusable for this kind of high-power and high-efficiency application. This letter deals with the dynamic behaviour of state-of-the-art high-power IR-LEDs ($I_{max(peak)} = 5$ A). In the first part the theoretical response of such LEDs is described and compared with actual measurements. The second part deals with a novel LED drive circuit, especially suitable for high-current LEDs, to achieve a significant reduction in the optical rise and fall time to enable ns-pulse operation required for fast TOF-systems.

Manuscript received March 3, 2014; revised May 9, 2014; accepted July 2, 2014. Date of publication July 9, 2014; date of current version August 28, 2014.

H. Halbritter, C. Jäger, M. Schwind, and F. Möllmer are with OSRAM Opto Semiconductors, Regensburg 93055, Germany (e-mail: hubert.halbritter@osram-os.com; claus.jaeger@osram-os.com; michael.schwind@osram-os.com; frank.moellmer@osram-os.com).

R. Weber is with OSRAM Opto Semiconductors, Inc., Sunnyvale, CA 94086 USA (e-mail: rolf.weber@osram-os.com).

Color versions of one or more of the figures in this letter are available online at http://ieeexplore.ieee.org.

Digital Object Identifier 10.1109/LPT.2014.2336732

II. Theory

To evaluate the time-domain transient behaviour of state-of-the-art multi-quantum-well (MQW) LEDs we follow the theoretical model for double-heterostructure LEDs [5]–[7]. The relationship between the injected carrier concentration n, the optical output P_{opt} (characterized by the radiative recombination rate $R_{rec} \sim P_{opt}$) and the electrical pulse current I_{pulse} (modelled via the carrier injection rate into the quantum wells (QWs), $R_{in} \sim I_{pulse}$) is governed by the rate equation (neglecting any non-radiative recombination process):

$$\frac{dn}{dt} = R_{in}(t) - R_{rec}(t). \tag{1}$$

The carrier injection rate into the QW (with thickness d_{QW}, area A_{QW}, injected current density $J = I_{pulse}/A_{QW}$ and e_0 as the elementary charge) is given by:

$$R_{in} = \frac{J}{e_0 d_{QW}}. \tag{2}$$

The radiative recombination rate R_{rec} can be modelled as a bi-molecular recombination [5]

$$R_{rec} = Bn\,(p_0 + n), \tag{3}$$

with B as radiative recombination constant and p_0 as doping concentration in the active layer. Further conditions are: Equal carrier concentration inside the MQWs, negligible carrier transport times and no photon recycling within the structure. This is also assumed for the 850 nm IR-LED SFH 4232 (1 mm^2 die) used in this experiment (and no doping inside the active layers ($p_0 = 0$)).

A. Optical Rise Time

For modelling the optical rise time a step-response of the LED forward current I_{pulse} is assumed. At first the depletion capacitance C_{depl} of the LED is charged (we will neglect this initial turn-on delay in the further discussion). Afterwards the MQWs get filled with carriers and radiative recombination sets in [8]. The time when radiation starts is defined as $t = 0$ in the following Eq.

The optical turn-on transient behaviour $P_{opt}(t)$ is the solution for the Eq. (1) (with $p_0 = 0$) and can be expressed as [5]

$$P_{opt}(t) \sim I_{pulse} \cdot tanh^2\left(\sqrt{k_{LED} I_{pulse}} \cdot t\right), \tag{4}$$

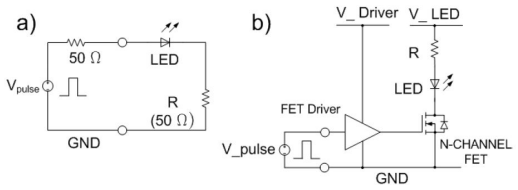

Fig. 1. Circuits to evaluate the intrinsic switching times of the LED. a) Traditional datasheet setup for low-current LEDs. b) Equivalent circuit for high-current LEDs.

with $k_{LED} = B/\left(e_0 d_{QW} A_{QW}\right)$ as an LED characteristic constant. Eq. (4) results in a 10 % to 90 % rise time of [5]

$$t_r = 1.49\frac{1}{\sqrt{k_{LED} \cdot I_{pulse}}} \sim 1.49\frac{1}{\sqrt{I_{pulse}}}. \tag{5}$$

B. Optical Fall Time

For modelling the optical turn-off transient behaviour a high-impedance model is used (considering that the LED is not discharged via an external circuit). It is also assumed that immediately prior to turn-off the carrier concentration (pulse current I_{pulse} resp. current density J) has reached a steady state. With this boundary condition and $J(t) = I_{pulse}(t) = 0$ at $t > 0$ (as well as $p_0 = 0$) the solution of Eq. (1) results in a time depending turn-off transient [5]

$$P_{opt}(t) \sim \frac{I_{pulse}}{\left(\sqrt{\frac{1}{k_{LED} \cdot I_{pulse}}} + t\right)^2}. \tag{6}$$

Eq. (6) gives a fall time of the optical signal (90 % to 10 %) of [5]

$$t_f = 2.11\frac{1}{\sqrt{k_{LED} \cdot I_{pulse}}} \sim 2.11\frac{1}{\sqrt{I_{pulse}}}. \tag{7}$$

Comparing Eq. (5) and (7) shows that in a high impedance drive circuit the LEDs intrinsic optical fall time is slower than the rise time (theoretically by a factor of $\sqrt{2}$), thus becoming the limiting factor in high-speed applications. In both cases the optical rise and fall times depend on the pulse current $\left(\sim 1/\sqrt{I_{pulse}}\right)$/current density $\left(\sim 1/\sqrt{J}\right)$.

C. Experimental Verification

To characterize the intrinsic LED switching time a high-impedance setup according to Fig. 1a) is employed. However, characterizing high current (> 1 A) LEDs makes this characterization method unpractical (mainly because of the required high voltage pulses, causing this setup to be no longer application relevant). A more applicable characterization method is the use of a high-impedance FET-based circuit. In this letter a setup according to Fig. 1b) with $R = 2.7\ \Omega$, a FET with fast rise/fall times (FDG 1024NZ and BLF573S for $>$ 5 A, both driven from a FET-driver (ISL 55110) with high drive voltage to achieve fast electrical rise/fall times, e.g. 8 V gate voltage) and a 850 nm IR-LED SFH 4232 is used. Due to the FETs leakage current the turn-on delay of the LED is reduced significantly. The setup has been verified to deliver the same optical rise and fall time as the conventional 50 Ω based setup in Fig. 1a). Additionally, the electrical rise and fall times (including the photodetector) are $\ll 2$ ns, thus not impacting the overall performance (verified by operating various LASERs instead of an LED).

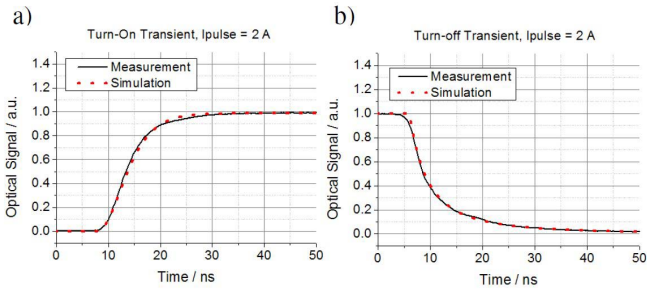

Fig. 2. a) Measurement and simulation according to Eq. (4) of the turn-on (rise time) behaviour. b) Measurement and simulation according to Eq. (6) of the turn-off (fall time) behaviour of the LED. Setup: According to Fig. 1b).

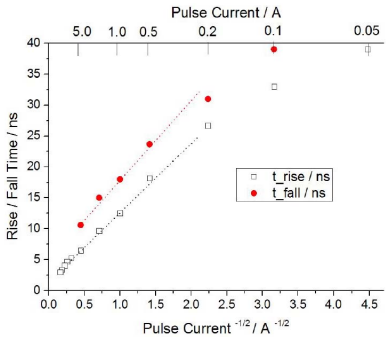

Fig. 3. Optical rise and fall time vs. LED pulse current of the 850 nm 1 mm^2 LED measured with a setup according to Fig. 1b). Please note that the datasheet limit is 5 A for I_{pulse}.

Fig. 2 presents the measured intrinsic optical rise and fall times of this LED at a 2 A pulse current. The pulse shape matches excellent with the theoretically derived pulse shape. From Eqs. (4) resp. (6) the LED characteristic parameter $k_{LED} \approx 1.5 \cdot 10^{16}\ \frac{1}{\mathrm{A \cdot s^2}}$ can be derived.

Fig. 3 present the dependence of the optical rise and fall time vs. the pulse current/current density. Here an excellent match with the theoretically predicted dependency $(1/\sqrt{I_{pulse}})$ can be seen as well. It is worth noting that outside of the typical current application range (0.5 A to 5 A), e.g. at low pulse currents the rise resp. fall time dependency tends to deviate from Eq. (4) and (6), indicating that non-radiative recombination becomes more dominant at very low currents [5].

III. Novel Drive Circuit

A. Optical Rise Time

Current peaking technique [2] is applied to reduce the optical rise time. This is done by adding a speed-up capacitance in parallel to the current-limiting resistor R in Fig. 1b). The peaking current during the turn-on phase also induces an optical peaking which can be shaped accordingly to create a fast optical rise time for short ns-pulses. However this circuit modification has no influence on the optical fall time which is usually the bottleneck, see also Eq. (5) and (7).

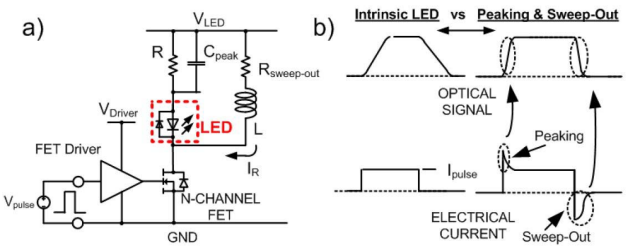

Fig. 4. a) LED drive circuit to create fast optical rise and fall times for ns-pulses (note that the IR-LED SFH 4232 already has a ESD protection diode inside the package). b) Physical principle applied: current peaking during the rising slope and active carrier sweep-out during the turn-off phase to reduce the optical rise and fall times.

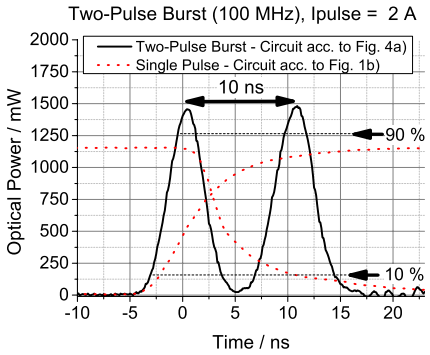

Fig. 5. Two-pulse burst with 100 MHz repetition rate. The optical rise and fall times are ∼2.6 ns ($I_{pulse} = 2$ A). For reference the same LED ($t_r = 10$ ns, $t_f = 14$ ns) is operated with standard drive circuit according to Fig. 1b) ($I_{pulse} = 2$ A). The difference in output power is caused by current peaking.

B. Optical Fall Time

To improve the optical fall time it is common to short-circuit the LED during the turn-off phase [3]. However when operating high-current MQW IR-LEDs with peak currents beyond 1 A this strategy is of limited value. At high currents a complete discharge of the MQW structure cannot be realized within a reasonable time (e.g. <3 ns) as the RC_{LED} time-constant delays the MQW discharge (junction capacitance C_{j0} is around 450 pF for this 1 mm^2 MQW LED). Instead an active solution needs to be employed which can be combined with the peaking principle. Here an inductor is used to discharge the LED with a reverse current I_R during the turn-off phase to achieve active carrier sweep-out.

C. Experimental Results

Fig. 4a) presents a circuit featuring both principles, current peaking during the turn-on phase and active sweep-out during the turn-off phase (see Fig. 4b) for illustration). The circuit requires no second pulse for the sweep-out path. A pure resistive sweep-out path ($L \sim 0$ nH) reduces the optical fall time from ∼15 ns to ∼10 ns (at 2 A pulse current). A more effective reduction is achieved by adding an inductive component which provides a sweep-out current I_R during the complete turn-off cycle (fall time). For our experimental setup we used the following component values: $R = 5.1\ \Omega$, $C_{peak} = 2.2$ nF (for current peaking to speed-up t_r) and $R_{sweep-out} = 3.4\ \Omega$, $L = 5.6$ nH for the carrier sweep-out path. Fig. 5 presents a 5 ns two-pulse optical burst signal. The same IR-LED (SFH 4232) as in Fig. 2 and 3, with a pulse current of 2 A was used. With this circuit the optical rise and fall times can be dramatically reduced to around 2.6 ns without an optical output power (LED efficiency) reduction. The short pulse reaches a $P_{opt(peak)} = 1400$ mW (see Fig. 5) vs. $P_{opt(100ns\ pulse)} = 1150$ mW for a 100 ns long pulse, both driven with 2 A. The slight increase in output power is caused by the peaking. Similar performance in terms of rise and fall times can be obtained at other drive currents by adapting the sweep-out current I_R.

This drive circuit works well for short ns-single pulses or bursts with low pulse counts and low overall duty cycle (like common for some TOF systems). The passive network (R, $R_{sweep-out}$, C_{peak}, L) needs to be tuned to the desired pulse shape and duration to achieve maximum optical efficiency (e.g. for LED: no power loss compared to DC operation). However, longer pulse trains cause high power dissipation in the passive components and intersymbol interference might become an issue. Thus for applications like data communication a good approach might require a more integrated solution (which can also reduce power consumption in the drive electronics).

IV. Conclusion

This letter evaluates the dynamic behaviour of high-power, high-current LEDs with MQW and surface textured thin-film structure. The experimentally obtained large-signal time response matches very well with the theory in terms of pulse shape as well as general dependency ($\sim 1/\sqrt{I_{pulse}}$). To significantly reduce the LEDs intrinsic optical rise and fall times a novel drive circuit is introduced which employs current peaking as well as an active carrier sweep-out technique, especially suitable for high-power, high-current LED's. As demonstrated, this technique is able to create 5 ns pulses with symmetrical optical rise and fall times of ∼2.6 ns (100 MHz) without sacrificing LED efficiency or output power.

References

[1] A. A. Dorrington, A. D. Payne, and M. J. Cree, "An evaluation of time-of-flight range cameras for close range metrology applications," in *Proc. Int. Archives Photogramm., Remote Sens. Spacial Inform. Sci.*, Jun. 2010, pp. 201–206.

[2] P. H. Binh, P. Renucci, V. G. Truong, and X. Marie, "Schottky-capacitance pulse-shaping circuit for high-speed light emitting diode operation," *Electron. Lett.*, vol. 48, no. 12, pp. 721–723, Jun. 2012.

[3] T. Kishi, H. Tanaka, Y. Umeda, and O. Takyu, "A high-speed LED driver that sweeps out the remaining carriers for visible light communications," *J. Lightw. Technol.*, vol. 32, no. 2, pp. 239–248, Jan. 15, 2014.

[4] H. L. Minh *et al.*, "100-Mb/s NRZ visible light communications using a postequalized white LED," *Photon. Technol. Lett.*, vol. 21, no. 15, pp. 1063–1065, Aug. 1, 2009.

[5] R. Windisch *et al.*, "Large-signal-modulation of high-efficiency light-emitting diodes for optical communication," *IEEE J. Quantum Electron.*, vol. 36, no. 2, pp. 1445–1453, Dec. 2000.

[6] K. Ideda, S. Horiuchi, T. Tanaka, and W. Susaki, "Design parameters of frequency response of GaAs—(Ga,Al)As double heterostructure LED's for optical communications," *IEEE Trans. Electron Devices*, vol. ED-24, no. 7, pp. 1001–1005, Jul. 1977.

[7] T. P. Lee and A. G. Dentai, "Power and modulation bandwidth of GaAs-AlGaAs high-radiance LED's for optical communication systems," *IEEE J. Quantum Electron.*, vol. QE-14, no. 3, pp. 150–159, Mar. 1978.

[8] T. P. Lee, "Effect of junction capacitance on the rise time of LED's and on the turn-on delay of injection lasers," *Bell Syst. Tech. J.*, vol. 54, no. 1, pp. 53–68, Jan. 1975.